AMERICAN UNIVERSITY OF BEIRUT

MODEL REFERENCE ADAPTIVE CONTROL FOR A TWO-WHEELED ROBOT

by
HUSSEIN ALJLAILATY

A thesis
submitted in partial fulfillment of the requirements
for the degree of Master of Engineering
to the Department of Mechanical Engineering
of the Faculty of Engineering and Architecture
at the American University of Beirut

Beirut, Lebanon
April 2019

AMERICAN UNIVERSITY OF BEIRUT

MODEL REFERENCE ADAPTIVE CONTROL FOR A TWO-WHEELED ROBOT

by

HUSSEIN ALJLAILATY

Approved by:

Dr. Daniel Asmar, Associate Professor — Advisor
Department of Mechanical Engineering

Dr. Naseem Daher, Assistant Professor — Co-advisor
Department of Electrical and Computer Engineering

Dr. Elie Shammas, Associate Professor — Member of Committee
Department of Mechanical Engineering

Date of thesis defense: April 25, 2019

AMERICAN UNIVERSITY OF BEIRUT

THESIS, DISSERTATION, PROJECT RELEASE FORM

Student Name: AlJlailaty Hussein Mohamad
Last First Middle

● Master's Thesis ○ Master's Project ○ Doctoral Dissertation

■ I authorize the American University of Beirut to: (a) reproduce hard or electronic copies of my thesis, dissertation, or project; (b) include such copies in the archives and digital repositories of the University; and (c) make freely available such copies to third parties for research or educational purposes.

☐ I authorize the American University of Beirut, to: (a) reproduce hard or electronic copies of it; (b) include such copies in the archives and digital repositories of the University; and (c) make freely available such copies to third parties for research or educational purposes
after : **One ---- year from the date of submission of my thesis, dissertation, or project.**
Two ---- years from the date of submission of my thesis, dissertation, or project.
Three ---- years from the date of submission of my thesis, dissertation, or project.

Hussein Jlailaty May 2, 2019

Signature Date

ACKNOWLEDGMENTS

Special thanks are for Professor *Daniel Asmar* who advised me throughout the master's program, not only in the technical issues, but also in the moral ones. It's a great pleasure that he accepts my sincere gratitude for his help and supervision.

My recognition and gratitude are addressed to those who helped in accomplishing the work – Vision and Robotics Lab namely Dr. *Naseem Daher*, lab managers and the shops' staff.

AN ABSTRACT OF THE THESIS OF

Hussein Aljlailaty for Master of Engineering
Major: Mechanical Engineering

Title: Model Reference Adaptive Control for a Two-Wheeled Robot

In this thesis, a model reference adaptive controller (MRAC) is developed for a two-wheeled mobile robot (TWMR). The inverted pendulum by nature is an unstable system and may be subjected to severe disturbances either in environment, (flat, tilted or bumped surfaces), or in load characteristics. The objective of the controller is to keep the TWMR in the upright position and prevent it from tipping over when subjected to either unexpected impulses or shifted weights along its interior body (IB). The non-linear mathematical model for the robot is formulated in an appropriate way to prove applicability of the proposed MRAC. Knowing that this a non-linear single-input multi-output (SIMO) platform, the proposed adaptive controller should handle the non-linearities with no attempt for linearization and inherently deal with SIMO systems. Experimental results validate the effectiveness of the proposed method.

CONTENTS

ILLUSTRATIONS

CHAPTER I

INTRODUCTION

A. Survey

Two wheeled self-balancing vehicle based on the concept of an inverted pendulum is built by researchers at the industrial electronics laboratory. SEGWAY PT is such a one machine developed by Dean Kamen, now commercially obtainable as a battery-powered electric vehicle in the market. Researchers and engineers are working to develop techniques to make a dynamically stable system and to guarantee desired performance and robust solution. Many methods are applied and tested on this system platform. Dual-PID and LQR control techniques are designed and tested in Simulink and analyzed for vertical balance and position control . There are many past studies about the stabilization and optimization of two-wheeled inverted pendulum robots. They are state feedback control with pole placement method, Proportional-Integral-Derivative (PID) and Proportional-Derivative(PD) controllers, LQR, Model Predictive Control (MPC) . Kalman filtering and PID algorithm is used for a two wheeled car. PI control is not satisfactory for a two wheeled self-balancing robot to act in a real time application. Different new research works has found on inverted pendulum techniques in the implementation of bipedal locomotion.

This dissertation is on the design of a two balancing wheel robot. A two wheeled robot is simply a robot that operates on two wheels. This is a topic that has attracted so much attention in the field of control engineering because of its nature as a natural unstably

The JOE in [3], simplified the controller design by decoupling the vehicle dynamics into two subsystems, yaw motion and pitch motion. Then a simple state feedback algorithm by pole placement was implemented for each of the subsystems. Deng et al. in [4] designed a feedback controller to study the behavior of the two-wheeled mobile robot in different dynamic environments. The proposed controller was based on a Lyapunov function candidate, where stability can be guaranteed. The candidate function that was used depends on the Euclidean distance and the magnitude of the relative velocity between the robot and the target. No investigation was done on the effect of changing the direction of applied disturbances for safe operations during such cases. In fact, this has not caused any failure in our self-tuned controller design due to online parameter estimation of the plant. Goher et al. in [5] investigated controlling a TWMR with a payload placed at variable positions on the vehicle body. A fuzzy logic controller was designed and implemented using two scenarios; The first is when the payload is at variable positions on the body; and the second is when the payload is in continuous sliding motion along the body. An external disturbance is applied to the robot to test the robustness of the developed controllers. Since this controller isn't adaptive it should be tuned each time the scenario changed. Nguyen et al in [6], propose to balance the two-wheeled mobile robot by designing an H_∞ robust controller (full order controller).

The results showed that the quality of the controller is guaranteed, even after reduction of the robust controller from sixth order to third order. Improvements in their controller should be done to cope with various working environments. Xu el al in [7] present the mathematical model of a two-wheeled inverted pendulum mobile robot in an attempt to design and analyze the control system. The controller implemented was a linear

C. Thesis Objectives

To cope with this problem of uncertainty, a novel controller for the robot Figure 3 is designed using a model reference adaptive controller. The main contributions this proposal presents are as follows.

- First, no linearization of the dynamic model was attempted aiming at keeping all unmodeled dynamics observable.
- Second, the anticipated adaptive controller was proven to be asymptotically stable using the Lyapunov stability theory.
- Third, the proposed controller has been proficiently implemented and tested using a low-cost off-the-shelf microcontroller.

CHAPTER II

HARDWARE DESIGN

This chapter discusses the robot hardware which includes the robot chassis, the drive system, actuators, sensors and the controller.

A. The Robot Chassis

The robot chassis is built of wood plates. There are two side steel threaded rods where three more plates between the other two side rods are held. The three middle plates made from plywood form three platforms which have the duty of holding the circuitry of the robot and actuators. The height of the platforms can be adjusted by moving the plates up and down the threaded rods. This is down to adjust the height of the center of mass of the robot and workout height for smoother control of the robot. A third small wheel was initially put in the robot to hold the robot up before the final control was implemented. The body of the robot has got a rectangular shape of mass 1.114Kg. The spacing between the plywood is adjustable and the platforms can be reduced or increased as required. The height of the robot is fixed to the length of the two steel rods. The height can only be increased by replacing the side rods with longer ones. Below is a table of the robot specifications:

Notation	Description	value
$\boldsymbol{M_p}$	Mass of pendulum	1.1140 kg
$\boldsymbol{l}$	Length from center of wheel to center of pendulum	63.68 mm
$\boldsymbol{I_p}$	Inertia of Pendulum	0.0032968 kg-m^2
$\boldsymbol{r}$	Radius of Wheel	49 mm
$\boldsymbol{M_w}$	Mass of Wheel	0.1011 kg
$\boldsymbol{I_w}$	Inertia of Wheel	0.00013956 kg-m^2
$\boldsymbol{K_m}$	Motor Torque Constant	0.0104 N.m/A
$\boldsymbol{K_e}$	Back EMF Constant	0.0104 V/rad-sec
$\boldsymbol{R}$	Internal Resistance of Motor	3.2 Ω

Table 1 – Robot Properties

B. Controller Board

1. Microcontroller

The main board of the robot consists of an Atmel 8-bit ATmega1284P AVR microcontroller running at 10MHz and with 128KB flash, 16KB RAM and 4KB EEProm. The board also contains an FTDI USB to Serial converter chip, the FT230X. This chip can be used for programming as well as Serial debugging.

The onboard 6-axis IMU is an MPU-6050, which is connected to the microcontroller using the I2C bus. This digital IMU contains a 3-axis accelerometer and a 3-axis gyroscope, and when combined with a Kalman filter it gives you very stable angle readings.

The fabrication of most accelerometers and gyroscopes today, use micro-electromechanical technology (MEMS). Mechanical functions and silicon wafers are placed on the same micrometer silicon substrate.

3. Sensor Data Fusion

Merging data from both accelerometers and gyroscopes serves to gain the best from both sensors. The strategy to accomplish this is called sensor fusion technology. Sensor fusion is usually accomplished by either Kalman or complementary filters. Both filters aim at reducing the uncertainty found in each sensor alone and increase the accuracy of the data from combining both.

The Kalman filter Figure 6, keeps track of the estimated state of the system and the variance or uncertainty of the estimated states. The states are updated using a state transition model and measurements. $\hat{x}_{k/k-1}$ denotes the estimate of the state at time step k before the kth measurement y_k has been considered, where $\hat{P}_{k/k-1}$ is the corresponding uncertainty.

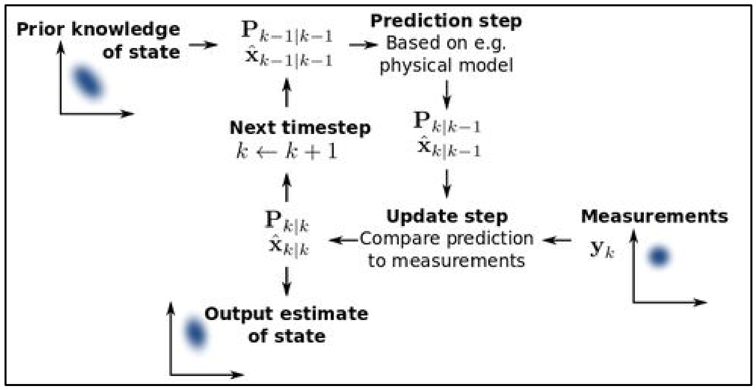

Figure 6 Kalman Filter (Image Source: Wikipedia)

The algorithm works in a two-step process. In the prediction step, the Kalman filter produces estimates of the current state variables, along with their uncertainties. Once the outcome of the next measurement (necessarily corrupted with some amount of error, including random noise) is observed, these estimates are updated using a weighted average, with more weight being given to estimates with higher certainty. The algorithm is recursive. It can run in real-time, using only the present input measurements and the previously calculated state and its uncertainty matrix; no additional past information is required.

4. Experimental Setup

The only input to the system is the analog voltage applied to the two DC motors used to drive the wheels, while the output of concern is the vertical angle of deflection of the TWMR. In order to test the controller in real-time, Simulink Desktop Real-Time Windows target by Simulink, which provides a real-time kernel for executing Simulink models was used. The key features of the Real-Time Windows target from Simulink include:

- Real-Time closed-loop execution of Simulink models.
- Signal Visualization and parameter tuning while model is running.
- Real-time performance approaching 20 KHz sample rate in Simulink external mode.

A duplex connection using the RS-232 interface protocol between the robot and the Real-time Simulink model is established. Data sent to the robot consists of:

- Forward, backward and left and right steering commands from the joystick after being conditioned (a discrete second-order low pass filter to the outputs of the joystick are applied to filter the high rate changing commands from the joystick) in the Simulink model.
- Motor voltages, which are sent as PWM (pulse-width modulation) could be used directly by the onboard DC motor driver on the robot.
- Leading and trailing data sent with the output stream to enable reliable data interconnection (a header and checksum were added to the beginning and trailing edge of the sentence to be sent respectively) between the robot and the Simulink model.

CHAPTER III

CONTROLLER DESIGN

A. Adaptive Controller

Intuitively, an adaptive controller is a controller that can modify its behavior in response to changes in the dynamics of the process and the character of the disturbances. Therefore, an adaptive controller is one with adjustable parameters and with a mechanism to adjust those parameters. An adaptive controller can be thought of as having two loops.

One loop is a normal feedback with a process and a controller. The other loop is the parameter adjustment loop. Figure 7 shows a block diagram of an adaptive system.

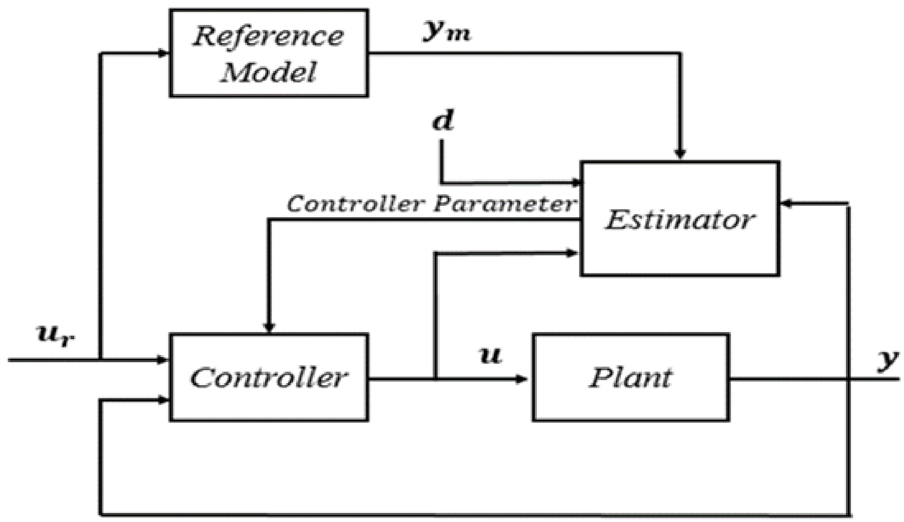

Figure 7 Block Diagram of Adaptive Controller

The model-reference adaptive system is an important adaptive controller. It may be regarded as an adaptive system in which the desired performance is expressed in terms of a reference model system, which gives the desired response with respect to a reference command. The system has a feedback loop that changes the parameters of the controller. The parameters are changed on the basis of the feedback from the error, which is the difference between the output of the system and the output of the reference model. The ordinary feedback loop is called the inner loop and the parameter adjustment loop is called the outer loop. The mechanism for adjusting the parameters is achieved by two ways. By using the gradient method or by using the stability theory.

The stability method used in this thesis is the Lyapunov stability theory. We first derive a differential equation for the error, $= y - y_m$. The differential equation contains the adjustable parameters. We then attempt to find a Lyapunov function and an adaptation mechanism such that the error will go to zero.

When using the Lyapunov theory we usually find that dV/dt is usually negative semi-definite. The procedure is to determine the error equation and the Lyapunov function with a bounded second derivative. Stability theory is then used to show boundedness and that the error goes to zero.

B. Mathematical Formulation

1. Dynamic Model of the TWMR

The robot is modelled as two rigid bodies, with no-slip rolling contact and a simple motor model. A polynomial style approximation of the dynamics is used to capture some of the nonlinearities, while keeping the controller design tractable. Using Newtons second law of motion, the sum of forces on the left wheel in the horizontal x-direction Figure 8 is $F_x = M_w\ddot{x} = H_{fL} - H_L$, where H_{fL} is the horizontal friction force, H_L is the horizontal force applied on the center of the left wheel, and M_w is the mass of the wheel.

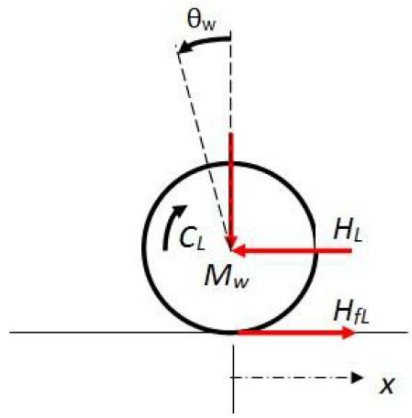

Figure 8 Left Hand Wheel

The sum of moments around the center of the wheel yields $M_w = I_w\ddot{\theta}_w = C_L - H_{fL}r$, where C_L is the moment applied by the motor on the left wheel, and r and I_w are the radius and moment of inertia of the wheel, respectively. Applying Newtons law of motion, the sum of forces in the horizontal direction on the chassis of the robot (Fig. 3) yields:

$$M_p\ddot{x} = (H_L + H_R) - Mpl\ddot{\theta}pcos(\theta)p + Mpl\dot{\theta}^2 sin(\theta p)$$

where $H_L + H_R$ is the total horizontal force applied on the chassis, θ_p represents the vertical angle of deflection of the robot, and M_p and l represent the mass and length of the pendulum, respectively. The sum of moments around the center of mass of the pendulum is $M = I_p\ddot{\theta}_p$ resulting in:

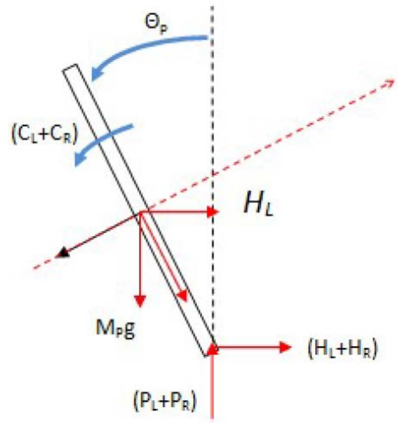

Figure 9 Free-Body Diagram of the Chassis

$$I_p\ddot{\theta} = (H_L + H_R)lcos(\theta_p) - (P_L + P_R)lsin(\theta_p) - (C_L + C_R)$$

where $P_L + P_R$ represent the total vertical force applied on the chassis, and I_p the moment of inertia of the pendulum.

1. Overview

For a two-wheeled mobile robot we have the two equations, (1) and (2) that govern the dynamics of motion. As can be easily seen, they are both second order coupled non-linear equations.

$$(\boldsymbol{I_p} + \boldsymbol{M_p}\boldsymbol{l}^2)\ddot{\boldsymbol{\theta}}_{\boldsymbol{p}} - \frac{2\boldsymbol{k_m}\boldsymbol{k_e}}{\boldsymbol{R}}\frac{\dot{\boldsymbol{x}}}{\boldsymbol{r}} + \frac{2\boldsymbol{k_m}}{\boldsymbol{R}}\boldsymbol{V_a} + \boldsymbol{M_p}\boldsymbol{glsin}\boldsymbol{\theta_p} = -\boldsymbol{M_p}\boldsymbol{l}\ddot{\boldsymbol{x}}\boldsymbol{cos}\boldsymbol{\theta_p} \qquad 1)$$

$$\frac{2\boldsymbol{k_m}}{\boldsymbol{Rr}}\boldsymbol{V_a} = \left(2\boldsymbol{M_w} + \frac{2\boldsymbol{I_w}}{\boldsymbol{r}^2} + \boldsymbol{M_p}\right)\ddot{\boldsymbol{x}} + \frac{2\boldsymbol{k_m}\boldsymbol{k_e}}{\boldsymbol{Rr}^2}\dot{\boldsymbol{x}} + \boldsymbol{M_p}\boldsymbol{l}\ddot{\boldsymbol{\theta}}_{\boldsymbol{p}}\boldsymbol{cos}\boldsymbol{\theta_p} - \boldsymbol{M_p}\boldsymbol{l}\dot{\boldsymbol{\theta}}_{\boldsymbol{p}}{}^2\boldsymbol{sin}\boldsymbol{\theta_p} \qquad 2)$$

The approach I took earlier was to linearize these dynamic equations around an equilibrium point which allows us to apply the Indirect Self Tuning Regulator adaptive controller capable of preventing the robot from tipping over when subjected to uncertain or unexpected disturbances. The main drawback of the ISTR regulator I used earlier is that it is solely used for linear single-input single-output (SISO) types of dynamic systems. Knowing that my experimental platform is a non-linear multi-input multi output (MIMO) type, I had to linearize my system as mentioned above, and augment my controller with an additional integrator to deal with the MIMO problem encountered to achieve the desired motion. This issue promoted me to search for an adaptive controller that could handle both gaps: First, handle the non-linearity in my system with no attempt for linearization. Second, use an adaptive controller that inherently deals with MIMO type systems.

Of course, the aim of this research is to improve the quality of my adaptive controller by forcing the output tracking error to become asymptotically smaller, and more robust to system uncertainties and environmental disturbances. For this task I propose to use a model reference adaptive controller (MRAC) Figure 10 that will extend the applicability of the controller to multi-input multi-output type nonlinear systems having the following structure:

$$\dot{x} = Ax + B\Lambda(u + f(x))$$

3)

where $x \in \ R^n$ is the system state, $u \in \ R^m$ is the control input, and $B \in \ R^{n*m}$ is the known control matrix, while $A \in \ R^{n*n}$ and $\Lambda \in \ R^{m*m}$ are unknown constant matrices.

In addition, it is assumed that Λ is diagonal, its elements λ_i are strictly positive, and the pair $(A, B\Lambda)$ is controllable. The uncertainty in Λ is introduced to model control failures or modeling errors, in the sense that there may exist uncertain control gains, or the designer may have incorrectly estimated the system control effectiveness.

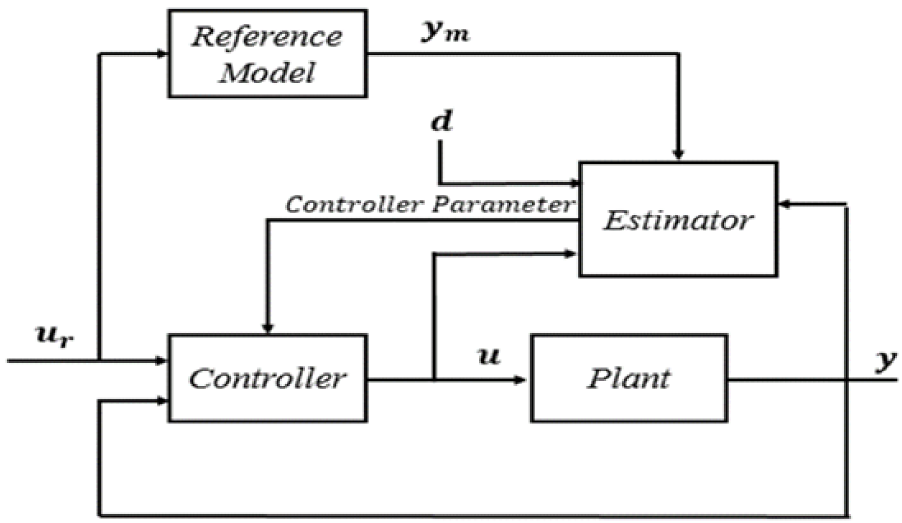

Figure 10 Adaptive Controller Block Diagram

The unknown possibly nonlinear vector-function $f(x): R^n \longrightarrow R^m$ represents the system matched uncertainty. It is assumed that each individual component $f_i(x)$ of $f(x)$ can be written as a linear combination of N locally Lipchitz-continuous basis functions $\varphi_i(x)$, with unknown constant coefficients. So, we write:

$$f(x) = \Theta^T \Phi(x) \quad 4)$$

where $\Theta \in R^{N*m}$is a constant matrix of unknown coefficients and $\Phi(x) = (\varphi_1(x) \dots \ \varphi_N(x)\ )^T \in\ R^n$ is the known regressor vector. We are interested in the design of a MIMO adaptive control law such that the system state x asymptotically tracks the state $x_{ref} \in\ R^n$ of the reference model (5):

$$\mathbf{\dot{x}_{ref}} = \mathbf{A_{ref}x_{ref}} + \mathbf{B_{ref}r(t)} \tag{5)}$$

where $A_{ref} \in R^{n*n}$ is Hurwitz, $B_{ref} \in R^{n*m}$, and $r(t)$ is the external command vector. Given any bounded command $r(t)$ the control input needs to be chosen such that the state tracking error:

$$\mathbf{e(t)} = \mathbf{x(t)} - \ \mathbf{x_{ref}(t)} \tag{6)}$$

globally uniformly asymptotically tends to zero, that is:

$$\lim_{t\to\infty} \left\| \boldsymbol{x}(\boldsymbol{t}) - \ \boldsymbol{x}_{\boldsymbol{ref}}(\boldsymbol{t}) \right\| = \mathbf{0} \tag{7)}$$

We consider the following control law:

$$\boldsymbol{u} = \widehat{\boldsymbol{K}}_x^T \boldsymbol{x} + \widehat{\boldsymbol{K}}_r^T \boldsymbol{r} - \widehat{\boldsymbol{\Theta}}^T \boldsymbol{\Phi}(\boldsymbol{x}) \tag{8)}$$

where $\widehat{K}_x \in R^{n*m}$, $\widehat{K}_r \in R^{m*m}$, $\widehat{\Theta} \in R^{N*n}$ are the estimates of the ideal unknown matrices K_x, K_r, and Θ respectively. These estimated parameters will be generated online through the inverse Lyapunov analysis. Substituting into the closed-loop dynamics, system dynamics can be written as:

$$\dot{\boldsymbol{x}} = \left(\boldsymbol{A} + \boldsymbol{B\Lambda}\widehat{\boldsymbol{K}}_x^{\boldsymbol{T}}\right)\boldsymbol{x} + \boldsymbol{B\Lambda}(\widehat{\boldsymbol{K}}_r^{\boldsymbol{T}}\boldsymbol{r} - \left(\widehat{\boldsymbol{\Theta}} - \boldsymbol{\Theta}\right)^{\boldsymbol{T}}\boldsymbol{\Phi}(\boldsymbol{x})) \tag{9}$$

We compute the closed-loop dynamics of the n-dimensional tracking error vector $e(t) = x(t) - x_{ref}(t)$ and:

$$\dot{\boldsymbol{e}} = \left(\boldsymbol{A} + \boldsymbol{B\Lambda}\widehat{\boldsymbol{K}}_x^{\boldsymbol{T}}\right)\boldsymbol{x} + \boldsymbol{B\Lambda}\left(\widehat{\boldsymbol{K}}_r^{\boldsymbol{T}}\boldsymbol{r} - \left(\widehat{\boldsymbol{\Theta}} - \boldsymbol{\Theta}\right)^{\boldsymbol{T}}\boldsymbol{\Phi}(\boldsymbol{x})\right) - \boldsymbol{A}_{\boldsymbol{ref}}\boldsymbol{x}_{\boldsymbol{ref}} - \boldsymbol{B}_{\boldsymbol{ref}}\boldsymbol{r}(\boldsymbol{t}) \tag{10}$$

We further get:

$$\begin{aligned}\dot{\boldsymbol{e}} = {} & \left(\boldsymbol{A}_{\boldsymbol{ref}} + \boldsymbol{B\Lambda}(\widehat{\boldsymbol{K}}_x^{\boldsymbol{T}} - \boldsymbol{K}_x)\right)\boldsymbol{x} - \boldsymbol{A}_{\boldsymbol{ref}}\boldsymbol{x}_{\boldsymbol{ref}} \\ & + \boldsymbol{B\Lambda}\left((\widehat{\boldsymbol{K}}_r - \boldsymbol{K}_r)\boldsymbol{r} - \left(\widehat{\boldsymbol{\Theta}} - \boldsymbol{\Theta}\right)^{\boldsymbol{T}}\boldsymbol{\Phi}(\boldsymbol{x})\right) \\ & = \boldsymbol{A}_{\boldsymbol{ref}}\boldsymbol{e} \\ & + \boldsymbol{B\Lambda}\left((\widehat{\boldsymbol{K}}_x - \boldsymbol{K}_x)^{\boldsymbol{T}}\boldsymbol{x} + (\widehat{\boldsymbol{K}}_r - \boldsymbol{K}_r)^{\boldsymbol{T}}\boldsymbol{r} - \left(\widehat{\boldsymbol{\Theta}} - \boldsymbol{\Theta}\right)^{\boldsymbol{T}}\boldsymbol{\Phi}(\boldsymbol{x})\right)\end{aligned} \tag{11}$$

Let $\Delta K_x = \widehat{K}_x - K_x$, $\Delta K_r = \widehat{K}_r - K_r$, and $\Delta\Theta = \widehat{\Theta} - \Theta$ represent the parameter estimation errors. The tracking error dynamics becomes:

$$\dot{\boldsymbol{e}} = \boldsymbol{A}_{ref}\boldsymbol{e} + \boldsymbol{B}\boldsymbol{\Lambda}(\Delta\boldsymbol{K}_x^T\boldsymbol{x} + \Delta\boldsymbol{K}_r^T\boldsymbol{r} - \Delta\boldsymbol{\Theta}^T\boldsymbol{\Phi}(\boldsymbol{x})) \qquad 12)$$

We introduce rates of adaptation: $\Gamma_x = \Gamma_x^T > 0$, $\Gamma_r = \Gamma_r^T > 0$, $\Gamma_\Theta = \Gamma_\Theta^T > 0$. Let us consider a quadratic Lyapunov function candidate in the form:

$$\begin{aligned}\boldsymbol{V}(\boldsymbol{e}, \Delta\boldsymbol{K}_x, \Delta\boldsymbol{K}_r, \Delta\boldsymbol{\Theta}) \\ = \boldsymbol{e}^T\boldsymbol{P}\boldsymbol{e} + \boldsymbol{tr}([\Delta\boldsymbol{K}_x^T\boldsymbol{\Gamma}_x^{-1}\Delta\boldsymbol{K}_x + \Delta\boldsymbol{K}_r^T\boldsymbol{\Gamma}_r^{-1}\Delta\boldsymbol{K}_r + \Delta\boldsymbol{\Theta}^T\boldsymbol{\Gamma}_{\boldsymbol{\Theta}}^{-1}\Delta\boldsymbol{\Theta}]\boldsymbol{\Lambda})\end{aligned} \qquad 13)$$

where $P = P^T > 0$ satisfies the algebraic Lyapunov equation:

$$\boldsymbol{P}\boldsymbol{A}_{ref} + \boldsymbol{A}_{ref}^T\boldsymbol{P} = -\boldsymbol{Q} \qquad 14)$$

for some $Q = Q^T > 0$. Then the time derivative of V evaluated along the error trajectories can be calculated as:

$$\begin{aligned}\dot{\boldsymbol{V}} = \dot{\boldsymbol{e}}^{\boldsymbol{T}}\boldsymbol{Pe} + \boldsymbol{e}^{\boldsymbol{T}}\boldsymbol{P}\dot{\boldsymbol{e}} + \boldsymbol{2tr}\left(\left[\Delta\boldsymbol{K}_x^{\boldsymbol{T}}\boldsymbol{\Gamma}_x^{-1}\dot{\hat{\boldsymbol{K}}}_x + \Delta\boldsymbol{K}_r^{\boldsymbol{T}}\boldsymbol{\Gamma}_r^{-1}\dot{\hat{\boldsymbol{K}}}_r + \Delta\boldsymbol{\Theta}^{\boldsymbol{T}}\boldsymbol{\Gamma}_{\boldsymbol{\Theta}}^{-1}\dot{\hat{\boldsymbol{\Theta}}}\right]\boldsymbol{\Lambda}\right) \\ = (\boldsymbol{A}_{ref}\boldsymbol{e} + \boldsymbol{B\Lambda}\left(\Delta\boldsymbol{K}_x^{\boldsymbol{T}}\boldsymbol{x} + \Delta\boldsymbol{K}_r^{\boldsymbol{T}}\boldsymbol{r} - \Delta\boldsymbol{\Theta}^{\boldsymbol{T}}\boldsymbol{\Phi}(\boldsymbol{x})\right))^{\boldsymbol{T}}\boldsymbol{Pe} + \boldsymbol{e}^{\boldsymbol{T}}\boldsymbol{P}(\boldsymbol{A}_{ref}\boldsymbol{e} \\ + \boldsymbol{B\Lambda}\left(\Delta\boldsymbol{K}_x^{\boldsymbol{T}}\boldsymbol{x} + \Delta\boldsymbol{K}_r^{\boldsymbol{T}}\boldsymbol{r} - \Delta\boldsymbol{\Theta}^{\boldsymbol{T}}\boldsymbol{\Phi}(\boldsymbol{x})\right) \\ + \boldsymbol{2tr}\left(\left[\Delta\boldsymbol{K}_x^{\boldsymbol{T}}\boldsymbol{\Gamma}_x^{-1}\dot{\hat{\boldsymbol{K}}}_x + \Delta\boldsymbol{K}_r^{\boldsymbol{T}}\boldsymbol{\Gamma}_r^{-1}\dot{\hat{\boldsymbol{K}}}_r + \Delta\boldsymbol{\Theta}^{\boldsymbol{T}}\boldsymbol{\Gamma}_{\boldsymbol{\Theta}}^{-1}\dot{\hat{\boldsymbol{\Theta}}}\right]\boldsymbol{\Lambda}\right) \\ = \boldsymbol{e}^{\boldsymbol{T}}\left(\boldsymbol{A}_{ref}\boldsymbol{P} + \boldsymbol{PA}_{ref}\right)\boldsymbol{e} \\ + \boldsymbol{2e}^{\boldsymbol{T}}\boldsymbol{PB\Lambda}\left(\Delta\boldsymbol{K}_x^{\boldsymbol{T}}\boldsymbol{x} + \Delta\boldsymbol{K}_r^{\boldsymbol{T}}\boldsymbol{r} - \Delta\boldsymbol{\Theta}^{\boldsymbol{T}}\boldsymbol{\Phi}(\boldsymbol{x})\right) \\ + \boldsymbol{2tr}\left(\left[\Delta\boldsymbol{K}_x^{\boldsymbol{T}}\boldsymbol{\Gamma}_x^{-1}\dot{\hat{\boldsymbol{K}}}_x + \Delta\boldsymbol{K}_r^{\boldsymbol{T}}\boldsymbol{\Gamma}_r^{-1}\dot{\hat{\boldsymbol{K}}}_r + \Delta\boldsymbol{\Theta}^{\boldsymbol{T}}\boldsymbol{\Gamma}_{\boldsymbol{\Theta}}^{-1}\dot{\hat{\boldsymbol{\Theta}}}\right]\boldsymbol{\Lambda}\right)\end{aligned} \quad 15)$$

which yields using the Lyapunov algebraic equation:

$$\begin{aligned}\dot{\boldsymbol{V}} = -\boldsymbol{e}^{\boldsymbol{T}}\boldsymbol{Qe} + [\boldsymbol{2e}^{\boldsymbol{T}}\boldsymbol{PB\Lambda}\Delta\boldsymbol{K}_x^{\boldsymbol{T}}\boldsymbol{x} + \boldsymbol{2tr}(\Delta\boldsymbol{K}_x^{\boldsymbol{T}}\boldsymbol{\Gamma}_x^{-1}\dot{\hat{\boldsymbol{K}}}_x\boldsymbol{\Lambda})] + [\boldsymbol{2e}^{\boldsymbol{T}}\boldsymbol{PB\Lambda}\Delta\boldsymbol{K}_r^{\boldsymbol{T}}\boldsymbol{r} \\ + \boldsymbol{2tr}(\Delta\boldsymbol{K}_r^{\boldsymbol{T}}\boldsymbol{\Gamma}_r^{-1}\dot{\hat{\boldsymbol{K}}}_r\boldsymbol{\Lambda})] + [-\boldsymbol{2e}^{\boldsymbol{T}}\boldsymbol{PB\Lambda}\Delta\boldsymbol{\Theta}^{\boldsymbol{T}}\boldsymbol{\Phi}(\boldsymbol{x}) \\ + \boldsymbol{2tr}(\Delta\boldsymbol{\Theta}^{\boldsymbol{T}}\boldsymbol{\Gamma}_{\boldsymbol{\Theta}}^{-1}\dot{\hat{\boldsymbol{\Theta}}}\boldsymbol{\Lambda})]\end{aligned} \quad (16)$$

and using the vector trace identity:

$$\boldsymbol{e}^{\boldsymbol{T}}\boldsymbol{PB\Lambda}\Delta\boldsymbol{K}_x^{\boldsymbol{T}}\boldsymbol{x} = \boldsymbol{tr}(\Delta\boldsymbol{K}_x^{\boldsymbol{T}}\boldsymbol{x}\boldsymbol{e}^{\boldsymbol{T}}\boldsymbol{PB\Lambda}) \quad 17)$$

$$\boldsymbol{e}^{\boldsymbol{T}}\boldsymbol{PB\Lambda}\Delta\boldsymbol{K}_r^{\boldsymbol{T}}\boldsymbol{r} = \boldsymbol{tr}(\Delta\boldsymbol{K}_r^{\boldsymbol{T}}\boldsymbol{r}\boldsymbol{e}^{\boldsymbol{T}}\boldsymbol{PB\Lambda}) \quad 18)$$

$$\boldsymbol{e}^{\boldsymbol{T}}\boldsymbol{PB\Lambda}\Delta\boldsymbol{\Theta}^{\boldsymbol{T}}\boldsymbol{\Phi}(\boldsymbol{x}) = \boldsymbol{tr}(\Delta\boldsymbol{\Theta}^{\boldsymbol{T}}\boldsymbol{\Phi}(\boldsymbol{x})\boldsymbol{e}^{\boldsymbol{T}}\boldsymbol{PB\Lambda}) \quad 19)$$

we obtain the following equation for the time derivative of $\boldsymbol{V}$:

$$\dot{\boldsymbol{V}} = -\boldsymbol{e}^{\boldsymbol{T}}\boldsymbol{Q}\boldsymbol{e} + \boldsymbol{2tr}(\Delta\boldsymbol{K}_{\boldsymbol{x}}^{\boldsymbol{T}}[\boldsymbol{\Gamma}_{\boldsymbol{x}}^{-\boldsymbol{1}}\dot{\hat{\boldsymbol{K}}}_{\boldsymbol{x}} + \boldsymbol{x}\boldsymbol{e}^{\boldsymbol{T}}\boldsymbol{P}\boldsymbol{B}]\boldsymbol{\Lambda}) + \boldsymbol{2tr}(\Delta\boldsymbol{K}_{\boldsymbol{r}}^{\boldsymbol{T}}[\boldsymbol{\Gamma}_{\boldsymbol{r}}^{-\boldsymbol{1}}\dot{\hat{\boldsymbol{K}}}_{\boldsymbol{x}} + \boldsymbol{2tr}(\Delta\boldsymbol{\Theta}^{\boldsymbol{T}}[\boldsymbol{\Gamma}_{\boldsymbol{\Theta}}^{-\boldsymbol{1}}\dot{\hat{\boldsymbol{\Theta}}} - \boldsymbol{\Phi}(\boldsymbol{x})\boldsymbol{e}^{\boldsymbol{T}}\boldsymbol{P}\boldsymbol{B}]\boldsymbol{\Lambda}) \quad 20)$$

If the adaptive law is selected as:

$$\dot{\hat{\boldsymbol{K}}}_{\boldsymbol{x}} = -\boldsymbol{\Gamma}_{\boldsymbol{x}}\boldsymbol{x}\boldsymbol{e}^{\boldsymbol{T}}\boldsymbol{P}\boldsymbol{B} \quad 21)$$

$$\dot{\hat{\boldsymbol{K}}}_{\boldsymbol{r}} = -\boldsymbol{\Gamma}_{\boldsymbol{r}}\boldsymbol{r}\boldsymbol{e}^{\boldsymbol{T}}\boldsymbol{P}\boldsymbol{B} \quad 22)$$

$$\dot{\hat{\boldsymbol{\Theta}}} = \boldsymbol{\Gamma}_{\boldsymbol{\Theta}}\boldsymbol{\Phi}(\boldsymbol{x})\boldsymbol{e}^{\boldsymbol{T}}\boldsymbol{P}\boldsymbol{B} \quad 23)$$

then the time derivative becomes:

$$\dot{\boldsymbol{V}} = -\boldsymbol{e}^{\boldsymbol{T}}\boldsymbol{Q}\boldsymbol{e} < \boldsymbol{0} \quad 24)$$

Therefore, the closed loop error dynamics are uniformly stable, and since

$$\dot{\boldsymbol{V}} = -\boldsymbol{e}^{\boldsymbol{T}}\boldsymbol{Q}\boldsymbol{e} < \boldsymbol{0} \quad 25)$$

is bounded, and so $\dot{V}$ is uniformly continuous. By Barbalat's lemma we have proven that the tracking error $e(t)$ tends to the origin asymptotically and

$$\lim_{t\to\infty}\left\|\boldsymbol{x(t)-\ x_{ref}(t)}\right\| = \mathbf{0}$$

26)

2. Non-linear Model derivation

Repeating equations (1) and (2) here:

$$(\boldsymbol{I_p}+\boldsymbol{M_p l^2})\boldsymbol{\ddot{\theta}_p}-\frac{\boldsymbol{2k_m k_e}}{\boldsymbol{R}}\frac{\boldsymbol{\dot{x}}}{\boldsymbol{r}}+\frac{\boldsymbol{2k_m}}{\boldsymbol{R}}\boldsymbol{V_a}+\boldsymbol{M_p g l sin\theta_p}=-\boldsymbol{M_p l\ddot{x} cos\theta_p}$$

27)

$$\frac{\boldsymbol{2k_m}}{\boldsymbol{Rr}}\boldsymbol{V_a}=\left(\boldsymbol{2M_w}+\frac{\boldsymbol{2I_w}}{\boldsymbol{r^2}}+\boldsymbol{M_p}\right)\boldsymbol{\ddot{x}}+\frac{\boldsymbol{2k_m k_e}}{\boldsymbol{Rr^2}}\boldsymbol{\dot{x}}+\boldsymbol{M_p l\ddot{\theta}_p cos\theta_p}-\boldsymbol{M_p l{\dot{\theta}_p}^2 sin\theta_p}$$

28)

Let $\boldsymbol{\beta}=\boldsymbol{I_p}+\boldsymbol{M_p l^2},\ \boldsymbol{\gamma}=\boldsymbol{2M_w}+\frac{\boldsymbol{2I_w}}{\boldsymbol{r^2}}+\boldsymbol{M_p}$ and $\boldsymbol{u}=\boldsymbol{V_a}$. Since $\boldsymbol{cos\theta_p}=\mathbf{1}-\frac{\boldsymbol{\theta_p}^2}{\mathbf{2}}+\cdots$ and $\boldsymbol{n\theta_p}=\boldsymbol{\theta_p}-\frac{\boldsymbol{\theta_p}^3}{\mathbf{6}}+\cdots$; then substituting in (27) and (28) gives:

$$\boldsymbol{\beta\ddot{\theta}_p}-\frac{\boldsymbol{2k_m k_e}}{\boldsymbol{Rr}}\boldsymbol{\dot{x}}+\frac{\boldsymbol{2k_m}}{\boldsymbol{R}}\boldsymbol{u}+\boldsymbol{M_p g l}\left(\boldsymbol{\theta_p}-\frac{\boldsymbol{\theta_p}^3}{\mathbf{6}}\right)=-\boldsymbol{M_p l\ddot{x}}\left(\mathbf{1}-\frac{\boldsymbol{\theta_p}^2}{\mathbf{2}}\right)$$

29)

$$\frac{\boldsymbol{2k_m}}{\boldsymbol{Rr}}\boldsymbol{u}=\boldsymbol{\gamma\ddot{x}}+\frac{\boldsymbol{2k_m k_e}}{\boldsymbol{Rr^2}}\boldsymbol{\dot{x}}+\boldsymbol{M_p l\ddot{\theta}_p}\left(\mathbf{1}-\frac{\boldsymbol{\theta_p}^2}{\mathbf{2}}\right)-\boldsymbol{M_p l{\dot{\theta}_p}^2}\left(\boldsymbol{\theta_p}-\frac{\boldsymbol{\theta_p}^3}{\mathbf{6}}\right)$$

30)

Leaving $\boldsymbol{\ddot{\theta}_p}$ and $\boldsymbol{\ddot{x}}$ on one side gives (31) and (32):

$$\ddot{\theta}_p = \frac{1}{\beta}\left(\frac{2k_m k_e}{Rr}\dot{x} - \frac{2k_m}{R}u - M_p g l\left(\theta_p - \frac{{\theta_p}^3}{6}\right) - M_p l\ddot{x}(1 - \frac{{\theta_p}^2}{2})\right) \quad 31)$$

$$\ddot{x} = \frac{1}{\gamma}\left(-\frac{2k_m k_e}{Rr^2}\dot{x} + \frac{2k_m}{Rr}u - M_p l\ddot{\theta}_p\left(1 - \frac{{\theta_p}^2}{2}\right) + M_p l{\dot{\theta}_p}^2(\theta_p - \frac{{\theta_p}^3}{6})\right) \quad 32)$$

Then working on the angular acceleration equation gives:

$$\ddot{\theta}_p = \frac{1}{\beta}\left(\frac{2k_m k_e}{Rr}\dot{x} - \frac{2k_m}{R}u - M_p g l\left(\theta_p - \frac{{\theta_p}^3}{6}\right) - M_p l\frac{1}{\gamma}\left(-\frac{2k_m k_e}{Rr^2}\dot{x} + \frac{2k_m}{Rr}u - M_p l\ddot{\theta}_p\left(1 - \frac{{\theta_p}^2}{2}\right) + M_p l{\dot{\theta}_p}^2(\theta_p - \frac{{\theta_p}^3}{6})\right)(1 - \frac{{\theta_p}^2}{2})\right) \quad 33)$$

which implies:

$$\ddot{\theta}_p - \frac{{M_p}^2 l^2}{\gamma\beta}\left(1 - \frac{{\theta_p}^2}{2}\right)^2\ddot{\theta}_p = \frac{1}{\beta}\left(\left(\frac{2k_m k_e}{Rr} + \frac{M_p l}{\gamma}\frac{2k_m k_e}{Rr^2}\left(1 - \frac{{\theta_p}^2}{2}\right)\right)\dot{x} - (\frac{2k_m}{R} + \frac{M_p l}{\gamma}\frac{2k_m}{Rr}\left(1 - \frac{{\theta_p}^2}{2}\right))u - M_p g l\left(\theta_p - \frac{{\theta_p}^3}{6}\right) - \frac{{M_p}^2 l^2}{\gamma}{\dot{\theta}_p}^2(\theta_p - \frac{{\theta_p}^3}{6})(1 - \frac{{\theta_p}^2}{2})\right) \quad (34)$$

and finally:

$$\ddot{\theta}_p = \frac{\frac{1}{\beta}(\frac{2k_m k_e}{Rr} + \frac{M_p l}{\gamma}\frac{2k_m k_e}{Rr^2}\left(1 - \frac{\theta_p{}^2}{2}\right))}{1 - \frac{M_p{}^2 l^2}{\gamma\beta}\left(1 - \frac{\theta_p{}^2}{2}\right)^2}\dot{x} - \frac{\frac{1}{\beta}(\frac{2k_m}{R} + \frac{M_p l}{\gamma}\frac{2k_m}{Rr}\left(1 - \frac{\theta_p{}^2}{2}\right))}{1 - \frac{M_p{}^2 l^2}{\gamma\beta}\left(1 - \frac{\theta_p{}^2}{2}\right)^2}u$$

$$- \frac{\frac{M_p g l}{\beta}\left(\theta_p - \frac{\theta_p{}^3}{6}\right)}{1 - \frac{M_p{}^2 l^2}{\gamma\beta}\left(1 - \frac{\theta_p{}^2}{2}\right)^2} - \frac{\frac{M_p{}^2 l^2}{\gamma\beta}\dot{\theta}_p{}^2(\theta_p - \frac{\theta_p{}^3}{6})(1 - \frac{\theta_p{}^2}{2})}{1 - \frac{M_p{}^2 l^2}{\gamma\beta}\left(1 - \frac{\theta_p{}^2}{2}\right)^2} \qquad 35)$$

Doing the same manipulation for $\ddot{x}$:

$$\ddot{x} = \frac{1}{\gamma}\left(-\frac{2k_m k_e}{Rr^2}\dot{x} + \frac{2k_m}{Rr}u - M_p l\ddot{\theta}_p\left(1 - \frac{\theta_p{}^2}{2}\right) + M_p l\dot{\theta}_p{}^2(\theta_p - \frac{\theta_p{}^3}{6})\right) \qquad 36)$$

which implies:

$$\ddot{x} = \frac{1}{\gamma}\left(-\frac{2k_m k_e}{Rr^2}\dot{x} + \frac{2k_m}{Rr}u\right.$$
$$- \frac{M_p l}{\beta}\left(\frac{2k_m k_e}{Rr}\dot{x} - \frac{2k_m}{R}u - M_p g l\left(\theta_p - \frac{\theta_p{}^3}{6}\right) - M_p l\ddot{x}(1\right. \qquad (37)$$
$$\left.\left. - \frac{\theta_p{}^2}{2})\right)\left(1 - \frac{\theta_p{}^2}{2}\right) + M_p l\dot{\theta}_p{}^2(\theta_p - \frac{\theta_p{}^3}{6})\right)$$

and finally:

$$\ddot{x} = \frac{-\frac{1}{\gamma}\left(\frac{2k_m k_e}{Rr^2} + \frac{M_p l}{\beta}\frac{2k_m k_e}{Rr}\left(1 - \frac{\theta_p{}^2}{2}\right)\right)}{1 - \frac{M_p{}^2 l^2}{\gamma\beta}\left(1 - \frac{\theta_p{}^2}{2}\right)^2}\dot{x}$$

$$+ \frac{\frac{1}{\gamma}\left(\frac{2k_m}{Rr} + \frac{M_p l}{\beta}\frac{2k_m}{R}\left(1 - \frac{\theta_p{}^2}{2}\right)\right)}{1 - \frac{M_p{}^2 l^2}{\gamma\beta}\left(1 - \frac{\theta_p{}^2}{2}\right)^2}u \qquad 38)$$

$$+ \frac{\frac{1}{\gamma}\frac{M_p{}^2 l^2 g}{\beta}\left(\theta_p - \frac{\theta_p{}^3}{6}\right)\left(1 - \frac{\theta_p{}^2}{2}\right)}{1 - \frac{M_p{}^2 l^2}{\gamma\beta}\left(1 - \frac{\theta_p{}^2}{2}\right)^2} + \frac{\frac{1}{\gamma}M_p l\dot{\theta}_p{}^2\left(\theta_p - \frac{\theta_p{}^3}{6}\right)}{1 - \frac{M_p{}^2 l^2}{\gamma\beta}\left(1 - \frac{\theta_p{}^2}{2}\right)^2}$$

The proposed multi-input multi-output type nonlinear system has the following structure:

$$\dot{x} = Ax + B\Lambda(u + f(x)) \qquad 39)$$

where $x \in R^n$ is the system state, $u \in R^m$ is the control input, and $B \in R^{n*m}$ is the known control matrix, while $A \in R^{n*n}$ and $\Lambda \in R^{m*m}$ are unknown constant matrices, also:

$$f(x) = \Theta^T\Phi(x) \qquad (40)$$

where $\Theta \in R^{n*m}$is a constant matrix of unknown coefficients and $\Phi(x) = (\varphi_1(x) \ldots \ \varphi_N(x)\ )^T \in R^n$ is the known regressor vector. We will now expand the fraction terms in the dynamic equations (35) and (38) in a Taylor series form around the equilibrium point; let:

$$\frac{\left(\frac{1}{r}+\frac{M_p l}{\beta}\left(1-\frac{{\theta_p}^2}{2}\right)\right)}{1-\frac{{M_p}^2 l^2}{\gamma\beta}\left(1-\frac{{\theta_p}^2}{2}\right)^2}=\left(a_0+a_1\theta_p+a_2\frac{{\theta_p}^2}{2}\right) \tag{41}$$

Expanding and solving equation (41) for the series terms:

$$\frac{1}{r}+\frac{M_p l}{\beta}\left(1-\frac{{\theta_p}^2}{2}\right)=\left(a_0+a_1\theta_p+a_2\frac{{\theta_p}^2}{2}\right)\left(1-\frac{{M_p}^2 l^2}{\gamma\beta}\left(1-\frac{{\theta_p}^2}{2}\right)^2\right) \tag{42}$$

$$\begin{aligned}\frac{1}{r}+\frac{M_p l}{\beta}-\frac{M_p l{\theta_p}^2}{2\beta}&\\ &=\left(a_0+a_1\theta_p+a_2\frac{{\theta_p}^2}{2}\right)\left(1-\frac{{M_p}^2 l^2}{\gamma\beta}+\frac{{M_p}^2 l^2{\theta_p}^2}{\gamma\beta}\right.\\ &\left.-\frac{{M_p}^2 l^2{\theta_p}^4}{4\gamma\beta}\right)\end{aligned} \tag{43}$$

$$\begin{aligned}\frac{1}{r}+\frac{M_p l}{\beta}-\frac{M_p l{\theta_p}^2}{2\beta}&\\ &=a_0-\frac{a_0{M_p}^2 l^2}{\gamma\beta}+\frac{a_0{M_p}^2 l^2{\theta_p}^2}{\gamma\beta}-\frac{a_0{M_p}^2 l^2{\theta_p}^4}{4\gamma\beta}+a_1\theta_p\\ &-\frac{a_1{M_p}^2 l^2\theta_p}{\gamma\beta}+\frac{a_1{M_p}^2 l^2{\theta_p}^3}{\gamma\beta}-\frac{a_1{M_p}^2 l^2{\theta_p}^5}{4\gamma\beta}+\frac{a_2{\theta_p}^2}{2}\\ &-\frac{a_2{M_p}^2 l^2{\theta_p}^2}{2\gamma\beta}+\frac{a_2{M_p}^2 l^2{\theta_p}^4}{2\gamma\beta}-\frac{a_2{M_p}^2 l^2{\theta_p}^6}{8\gamma\beta}\end{aligned} \tag{44}$$

Comparing left and right-hand sides gives:

$$a_0 = \frac{\frac{1}{r} + \frac{M_p l}{\beta}}{1 - \frac{{M_p}^2 l^2}{\gamma\beta}} \tag{45}$$

$$a_1 = 0 \tag{46}$$

$$a_2 = \frac{-\frac{a_0 {M_p}^2 l^2}{\gamma\beta} - \frac{M_p l}{2\beta}}{\frac{1}{2} - \frac{{M_p}^2 l^2}{2\gamma\beta}} \tag{47}$$

also let:

$$\frac{\left(\theta_p - \frac{{\theta_p}^3}{6}\right)\left(1 - \frac{{\theta_p}^2}{2}\right)}{1 - \frac{{M_p}^2 l^2}{\gamma\beta}\left(1 - \frac{{\theta_p}^2}{2}\right)^2} = b_0 + b_1\theta_p + b_2\frac{{\theta_p}^2}{2} + b_3\frac{{\theta_p}^3}{6} \tag{48}$$

Then:

$$\left(\theta_p - \frac{{\theta_p}^3}{6}\right)\left(1 - \frac{{\theta_p}^2}{2}\right) = \left(b_0 + b_1\theta_p + b_2\frac{{\theta_p}^2}{2} + b_3\frac{{\theta_p}^3}{6}\right)\left(1 - \frac{{M_p}^2 l^2}{\gamma\beta}\left(1 - \frac{{\theta_p}^2}{2}\right)^2\right) \tag{49}$$

Letting $\mu = \frac{{M_p}^2 l^2}{\gamma\beta}$ gives:

$$\boldsymbol{\theta_p - \frac{2{\theta_p}^3}{3} + \frac{{\theta_p}^5}{12}}$$

$$\boldsymbol{= b_0 - \mu b_0 + \mu b_0 {\theta_p}^2 - \frac{\mu b_0 {\theta_p}^4}{4} + b_1\theta_p - \mu b_1 \theta_p + \mu b_1 {\theta_p}^3}$$

$$\boldsymbol{- \frac{\mu b_1 {\theta_p}^5}{4} + b_2\frac{{\theta_p}^2}{2} - \mu b_2\frac{{\theta_p}^2}{2} + \mu b_2\frac{{\theta_p}^4}{2} - \mu b_2\frac{{\theta_p}^6}{8}} \tag{50}$$

$$\boldsymbol{+ (b_3 - \mu b_3)\frac{{\theta_p}^3}{6} + \mu b_3\frac{{\theta_p}^5}{6} - \frac{\mu b_3 {\theta_p}^7}{24}}$$

Comparing the left and right-hand sides we get:

$$\boldsymbol{b_0 = 0} \tag{51}$$

$$\boldsymbol{b_1 = \frac{1}{1-\mu}} \tag{52}$$

$$\boldsymbol{b_2 = 0} \tag{53}$$

$$\boldsymbol{b_3 = \frac{-\frac{2}{3} - \frac{\mu}{1-\mu}}{1-\mu}} \tag{54}$$

Assuming that:

$$\frac{(\theta_p - \frac{{\theta_p}^3}{6})}{1 - \frac{{M_p}^2 l^2}{\gamma\beta}\left(1 - \frac{{\theta_p}^2}{2}\right)^2} = c_0 + c_1\theta_p + c_2\frac{{\theta_p}^2}{2} + c_3\frac{{\theta_p}^3}{6} \tag{55}$$

We get:

$$\theta_p - \frac{{\theta_p}^3}{6} = c_0 - \mu c_0 + \mu c_0 {\theta_p}^2 - \frac{\mu c_0 {\theta_p}^4}{4} + c_1\theta_p - \mu c_1\theta_p + \mu c_1 {\theta_p}^3 - \frac{\mu c_1 {\theta_p}^5}{4} + c_2\frac{{\theta_p}^2}{2} - \mu c_2\frac{{\theta_p}^2}{2} + \mu c_2\frac{{\theta_p}^4}{2} - \mu c_2\frac{{\theta_p}^6}{8} + (c_3 - \mu c_3)\frac{{\theta_p}^3}{6} + \mu c_3\frac{{\theta_p}^5}{6} - \frac{\mu c_3 {\theta_p}^7}{24} \tag{56}$$

Which by comparing both sides yield:

$$c_0 = 0 \tag{57}$$

$$c_1 = \frac{1}{1 - \mu}$$

$$c_2 = 0 \tag{58}$$

$$c_3 = \frac{-\frac{1}{6} - \frac{\mu}{1 - \mu}}{1 - \mu} \tag{59}$$

The final form of the linear acceleration equation is:

$$\ddot{x} = -\frac{2k_m k_e}{\gamma R r}\left(a_0 + a_2\frac{{\theta_p}^2}{2}\right)\dot{x} + \frac{2k_m}{\gamma R}\left(a_0 + a_2\frac{{\theta_p}^2}{2}\right)u + \frac{{M_p}^2 l^2 g}{\gamma\beta}\left(b_1\theta_p + b_3\frac{{\theta_p}^3}{6}\right) + \frac{1}{\gamma}M_p l{\dot{\theta}_p}^2\left(c_1\theta_p + c_3\frac{{\theta_p}^3}{6}\right) \tag{60}$$

$$\ddot{x} = -\frac{2k_m k_e a_0}{\gamma R r}\dot{x} - \frac{k_m k_e a_2}{\gamma R r}\dot{x}{\theta_p}^2 + \frac{2k_m a_0}{\gamma R}u + \frac{k_m a_2}{\gamma R}u{\theta_p}^2 + g b_1\mu\theta_p + \frac{1}{6}b_3\mu g{\theta_p}^3 + \frac{1}{\gamma}M_p l c_1\theta_p{\dot{\theta}_p}^2 + \frac{1}{6\gamma}M_p l c_3{\theta_p}^3{\dot{\theta}_p}^2 \tag{61}$$

Now considering the angular acceleration equation:

$$\ddot{\theta}_p = \frac{\frac{2k_m k_e}{\beta R r}\left(1 + \frac{M_p l}{\gamma r}\left(1 - \frac{{\theta_p}^2}{2}\right)\right)}{1 - \frac{{M_p}^2 l^2}{\gamma\beta}\left(1 - \frac{{\theta_p}^2}{2}\right)^2}\dot{x} - \frac{\frac{2k_m}{\beta R}\left(1 + \frac{M_p l}{\gamma r}\left(1 - \frac{{\theta_p}^2}{2}\right)\right)}{1 - \frac{{M_p}^2 l^2}{\gamma\beta}\left(1 - \frac{{\theta_p}^2}{2}\right)^2}u - \frac{M_p g l\left(\theta_p - \frac{{\theta_p}^3}{6}\right)}{1 - \frac{{M_p}^2 l^2}{\gamma\beta}\left(1 - \frac{{\theta_p}^2}{2}\right)^2} - \frac{\frac{{M_p}^2 l^2}{\gamma}{\dot{\theta}_p}^2\left(\theta_p - \frac{{\theta_p}^3}{6}\right)\left(1 - \frac{{\theta_p}^2}{2}\right)}{1 - \frac{{M_p}^2 l^2}{\gamma\beta}\left(1 - \frac{{\theta_p}^2}{2}\right)^2} \tag{62}$$

let:

$$\frac{\left(1+\frac{M_p l}{\gamma r}\left(1-\frac{{\theta_p}^2}{2}\right)\right)}{1-\frac{{M_p}^2 l^2}{\gamma\beta}\left(1-\frac{{\theta_p}^2}{2}\right)^2}=\left(d_0+d_1\theta_p+d_2\frac{{\theta_p}^2}{2}\right) \tag{63}$$

Then:

$$1+\frac{M_p l}{\gamma r}\left(1-\frac{{\theta_p}^2}{2}\right)=\left(d_0+d_1\theta_p+d_2\frac{{\theta_p}^2}{2}\right)\left(1-\frac{{M_p}^2 l^2}{\gamma\beta}\left(1-\frac{{\theta_p}^2}{2}\right)^2\right) \tag{64}$$

$$\begin{aligned}1+\frac{M_p l}{\gamma r}-\frac{M_p l}{2\gamma r}{\theta_p}^2 \\ &= d_0-\frac{d_0{M_p}^2 l^2}{\gamma\beta}+\frac{d_0{M_p}^2 l^2{\theta_p}^2}{\gamma\beta}-\frac{d_0{M_p}^2 l^2{\theta_p}^4}{4\gamma\beta}+d_1\theta_p \\ &-\frac{d_1{M_p}^2 l^2\theta_p}{\gamma\beta}+\frac{d_1{M_p}^2 l^2{\theta_p}^3}{\gamma\beta}-\frac{d_1{M_p}^2 l^2{\theta_p}^5}{4\gamma\beta}+\frac{d_2{\theta_p}^2}{2} \\ &-\frac{d_2{M_p}^2 l^2{\theta_p}^2}{2\gamma\beta}+\frac{d_2{M_p}^2 l^2{\theta_p}^4}{2\gamma\beta}-\frac{d_2{M_p}^2 l^2{\theta_p}^6}{8\gamma\beta}\end{aligned} \tag{65}$$

After some tedious mathematical calculations below, we obtain:

$$d_0=\frac{1+\frac{M_p l}{\gamma r}}{1-\mu} \tag{66}$$

$$d_1=0 \tag{67}$$

$$d_2 = \frac{-\frac{M_p l}{2\gamma r} - \frac{{M_p}^2 l^2 \left(1 + \frac{M_p l}{\gamma r}\right)}{(1-\mu)\gamma\beta}}{\left(\frac{1}{2} - \frac{{M_p}^2 l^2}{2\gamma\beta}\right)} \qquad 68)$$

Also, taking $\frac{\left(\theta_p - \frac{{\theta_p}^3}{6}\right)}{1 - \frac{{M_p}^2 l^2}{\gamma\beta}\left(1 - \frac{{\theta_p}^2}{2}\right)^2} = c_1\theta_p + c_3\frac{{\theta_p}^3}{6}$ and $\frac{\left(\theta_p - \frac{{\theta_p}^3}{6}\right)\left(1 - \frac{{\theta_p}^2}{2}\right)}{1 - \frac{{M_p}^2 l^2}{\gamma\beta}\left(1 - \frac{{\theta_p}^2}{2}\right)^2} = b_1\theta_p + b_3\frac{{\theta_p}^3}{6}$ we get:

$$\begin{aligned}\ddot{\theta}_p = {} & \frac{2k_m k_e}{\beta R r}\left(d_0 + d_2\frac{{\theta_p}^2}{2}\right)\dot{x} - \frac{2k_m}{\beta R}\left(d_0 + d_2\frac{{\theta_p}^2}{2}\right)u \\ & - \frac{M_p g l}{\beta}\left(c_1\theta_p + c_3\frac{{\theta_p}^3}{6}\right) - \frac{{M_p}^2 l^2}{\gamma\beta}{\dot{\theta}_p}^2\left(b_1\theta_p + b_3\frac{{\theta_p}^3}{6}\right)\end{aligned} \qquad 69)$$

and finally:

$$\begin{aligned}\ddot{\theta}_p = {} & \frac{2k_m k_e d_0}{\beta R r}\dot{x} + \frac{k_m k_e d_2}{\beta R r}\dot{x}{\theta_p}^2 - \frac{2k_m d_0}{\beta R}u - \frac{k_m d_2}{\beta R}u{\theta_p}^2 - \frac{M_p g l c_1}{\beta}\theta_p \\ & - \frac{1}{6\beta}M_p g l c_3{\theta_p}^3 - \mu b_1\theta_p{\dot{\theta}_p}^2 - \frac{\mu}{6}b_3\,{\dot{\theta}_p}^2{\theta_p}^3\end{aligned} \qquad 70)$$

Letting $\boldsymbol{x} = \begin{bmatrix} x \\ \dot{x} \\ \theta_p \\ \dot{\theta}_p \end{bmatrix}$ be the state vector then we can write our non-linear equation in this form:

$$\dot{\boldsymbol{x}} = \boldsymbol{A}\boldsymbol{x} + \boldsymbol{B}\boldsymbol{\Lambda}(\boldsymbol{U} + \boldsymbol{f}(\boldsymbol{x})) \tag{71}$$

where $= \begin{pmatrix} \mathbf{0} & \mathbf{1} & \mathbf{0} & \mathbf{0} \\ \mathbf{0} & -\frac{\mathbf{2}k_m k_e a_0}{\gamma R r} & g b_1 \mu & \mathbf{0} \\ \mathbf{0} & \mathbf{0} & \mathbf{0} & \mathbf{1} \\ \mathbf{0} & \frac{\mathbf{2}k_m k_e d_0}{\beta R r} & \frac{-M_p g l c_1}{\beta} & \mathbf{0} \end{pmatrix}$, $\boldsymbol{B} = \begin{pmatrix} \mathbf{0} & \mathbf{0} \\ \frac{\mathbf{2}k_m a_0}{\gamma R} & \mathbf{0} \\ \mathbf{0} & \mathbf{0} \\ \mathbf{0} & -\frac{\mathbf{2}k_m d_0}{\beta R} \end{pmatrix}$, $\boldsymbol{U} = \begin{pmatrix} \boldsymbol{u} \\ \boldsymbol{u} \end{pmatrix}$.

Also, $\boldsymbol{f}(\boldsymbol{x}) = \boldsymbol{\Theta}^{T}\boldsymbol{\Phi}(\boldsymbol{x})$, $\boldsymbol{\delta} = -\frac{\mathbf{2}k_m d_0}{\beta R}$, $\boldsymbol{\epsilon} = \frac{\mathbf{2}k_m a_0}{\gamma R}$ where $\boldsymbol{\Phi}(\boldsymbol{x}) = \begin{pmatrix} \dot{x}{\theta_p}^{2} \\ u{\theta_p}^{2} \\ {\theta_p}^{3} \\ \theta_p {\dot{\theta}_p}^{2} \\ {\dot{\theta}_p}^{2} {\theta_p}^{3} \end{pmatrix}$ is the regression vector and the unknown parameters matrix.

To prove the concept discussed above, the plan is to do some simulation and then validate the simulations by implementing the controller on our two-wheeled robot platform and compare the results wit $\Theta = \begin{pmatrix} -\frac{k_m k_e a_2}{\gamma R r \epsilon} & \frac{k_m k_e d_2}{\beta R r \delta} \\ \frac{k_m a_2}{\gamma R \epsilon} & -\frac{k_m d_2}{\beta R \delta} \\ \frac{1}{6\epsilon} b_3 \mu g & -\frac{1}{6\beta\delta} M_p g l c_3 \\ \frac{1}{\gamma\epsilon} M_p l c_1 & -\frac{\mu b_1}{\delta} \\ \frac{1}{6\gamma\epsilon} M_p l c_3 & -\frac{\mu b_3}{6\delta} \end{pmatrix}$ h what has been previously done.

CHAPTER IV

SIMULATION AND RESULTS

Simulink Real-Time Windows Target was used as the main tool in simulating and verifying the results experimentally. The TWMR model was built and executed in real time while the controller was run from an ATMEL microcontroller equipped board.

$$\frac{\theta_{pref}}{\theta_{pcmd}} = \frac{w_n^2}{s^2 + 2\xi w_n + w_n^2} \quad 73)$$

which represent the desired command-to-reference behavior. Here x_{ref} and θ_{ref} are the reference position and pitch angle of the TWMR. x_{cmd} and θ_{cmd} the commanded position and pitch angle respectively, and $(w_n, \xi) = (10, 0.9)$ are the desired natural frequency, and the damping ratio. In state space form, the reference model dynamics of the TWMR can be easily written as:

$$\dot{x}_{ref} = A_{ref} x_{ref} + B_{ref} r(t) \quad 74)$$

$$\begin{pmatrix} \dot{x} \\ \ddot{x} \\ \dot{\theta}_p \\ \ddot{\theta}_p \end{pmatrix} = \begin{pmatrix} 0 & 1 & 0 & 0 \\ -w_n^2 & -2\xi w_n & 0 & 0 \\ 0 & 0 & 0 & 1 \\ 0 & 0 & -w_n^2 & -2\xi w_n \end{pmatrix} \begin{pmatrix} x \\ \dot{x} \\ \theta_p \\ \dot{\theta}_p \end{pmatrix} + \begin{pmatrix} 0 & 0 \\ w_n^2 & 0 \\ 0 & 0 \\ 0 & w_n^2 \end{pmatrix} r_{cmd}(t) \quad (76)$$

The MRAC design equations used in the simulation are:

- Open-loop plant: $\dot{x} = Ax + B\Lambda(u + \Theta^T \Phi(x))$
- Reference model: $\dot{x}_{ref} = A_{ref} x_{ref} + B_{ref} r(t)$
- Model matching conditions: $A + B\Lambda K_x^T = A_{ref},\ B\Lambda K_x^T = B_{ref}$
- Tracking error: $e = x - x_{ref}$

- Control input: $u = \hat{K}_x^T x + \hat{K}_r^T r - \hat{\Theta}^T \Phi(x)$
- Algebraic Lyapunov equation: $PA_{ref} + A_{ref}^T P = -Q$
- MIMO MRAC laws: $\dot{\hat{K}}_x = -\Gamma_x x e^T PB,$

$$\dot{\hat{K}}_r = -\Gamma_r r e^T PB$$

$$\dot{\hat{\Theta}} = \Gamma_\Theta \Phi(x) e^T PB$$

The design consists of symmetric positive-definite matrices Q, Γ_x, Γ_r and Γ_Θ , with the last three quantities representing adaptation rates for the parameters $\hat{K}_x$, $\hat{K}_r$ and $\hat{\Theta}$, respectively. After several iterations, we have selected the following data:

$$Q = \begin{pmatrix} 10000 & 0 & 0 & 0 \\ 0 & 10000 & 0 & 0 \\ 0 & 0 & 10000 & 0 \\ 0 & 0 & 0 & 10000 \end{pmatrix}$$

$$\Gamma_x = \begin{pmatrix} 100 & 0 & 0 & 0 \\ 0 & 100 & 0 & 0 \\ 0 & 0 & 100 & 0 \\ 0 & 0 & 0 & 100 \end{pmatrix}$$

$$\Gamma_r = \begin{pmatrix} 10 & 0 \\ 0 & 10 \end{pmatrix}$$

$$\Gamma_\theta = \begin{pmatrix} 10 & 0 & 0 & 0 & 0 \\ 0 & 10 & 0 & 0 & 0 \\ 0 & 0 & 10 & 0 & 0 \\ 0 & 0 & 0 & 10 & 0 \\ 0 & 0 & 0 & 0 & 10 \end{pmatrix}$$

Figure 12 shows the tracking performance of the adaptive MRAC controller. It Shows the system closed loop response in tracking a series of step input commands. The percentage overshoot and the rise-time are within the limits originally designed for.

As can be seen in Figure 13 the required control input stays within achievable and reasonable limits.

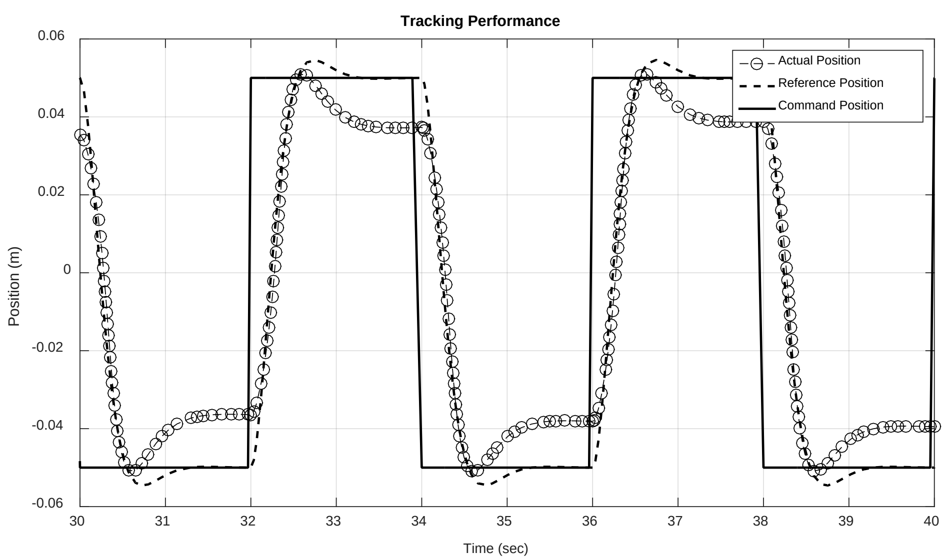

Figure 12 Tracking Performance

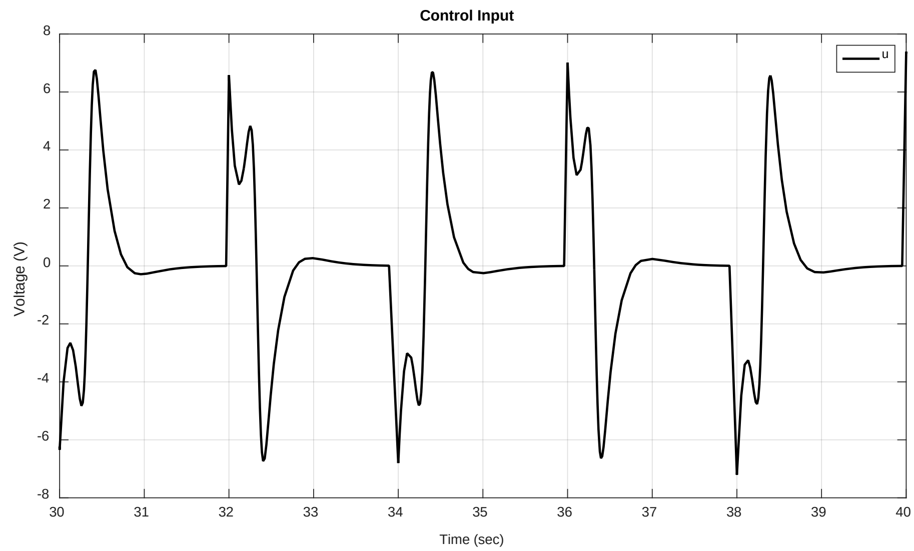

Figure 13 Control Input

The tracking error quickly dissipates which can be seen by observing the difference between the actual and the commanded input signal in Figure 14.

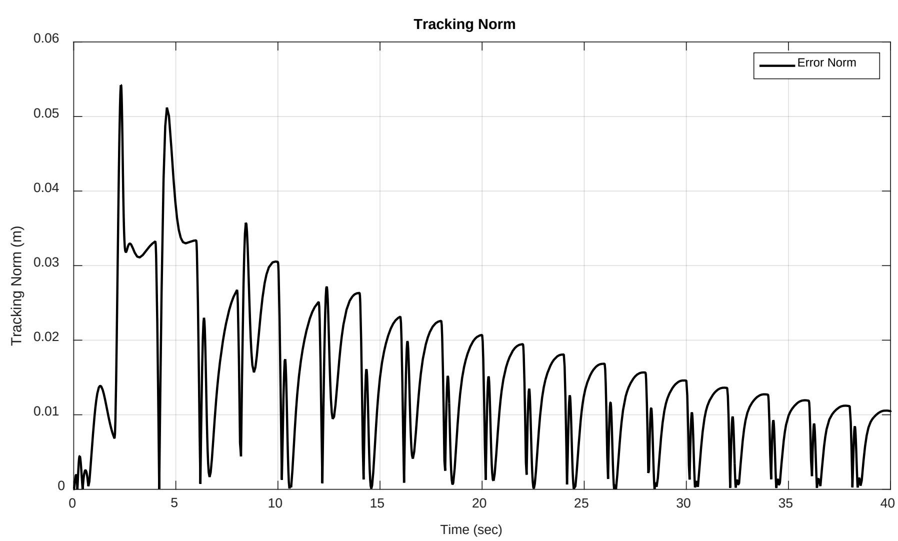

Figure 14 Tracking Norm

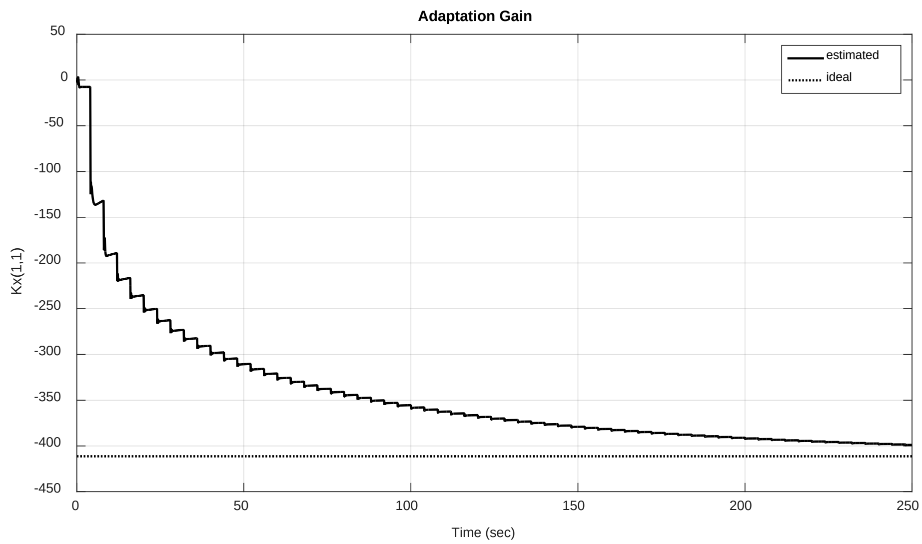

Figure 15 Evolution Time of Adaptive Gain

Parameter convergence in adaptive control depends on the persistency of excitation conditions. Basically, the external commands need to "persistently excite" the closed-loop system dynamics. This rule no longer holds for nonlinear systems and the general PE conditions are hard to verify numerically. It is interesting to observe that some of the feedback and feedforward gains $(\hat{K}_x, \hat{K}_r)$ converge to their true unknown values as shown in Figure 15 and Figure 16.

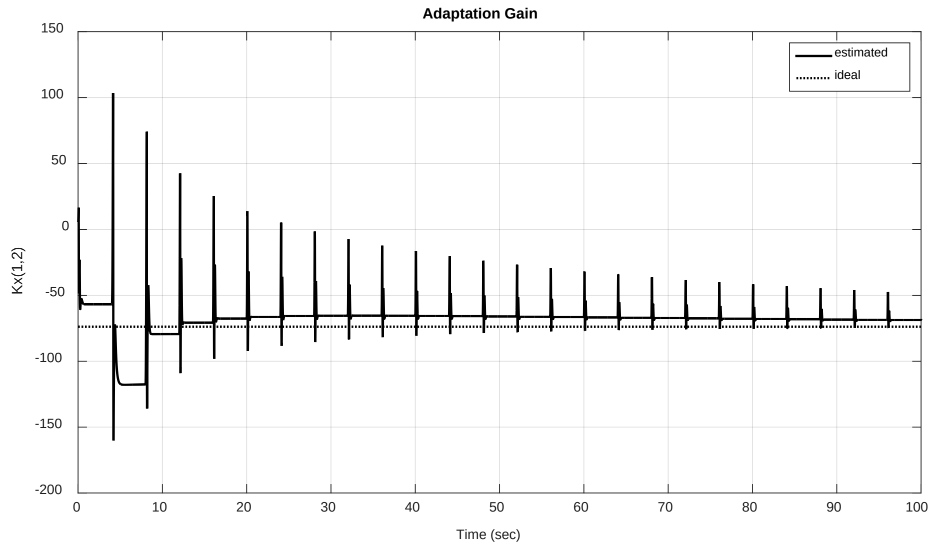

Figure 16 Evolution Time of Adaptive Gain

However, the estimated parameters $\left(\hat{\theta}_7, \hat{\theta}_8, \hat{\theta}_9, \hat{\theta}_{10}, \hat{\theta}_{11}, \hat{\theta}_{12}, \hat{\theta}_{13}, \hat{\theta}_{14}, \hat{\theta}_{15}, \hat{\theta}_{16}\right)$ that correspond to the nonlinear regressor components have dissimilar tendencies. Some are quite different from their ideal counterparts, while the third one does converge to its ideal value as shown in the figures below.

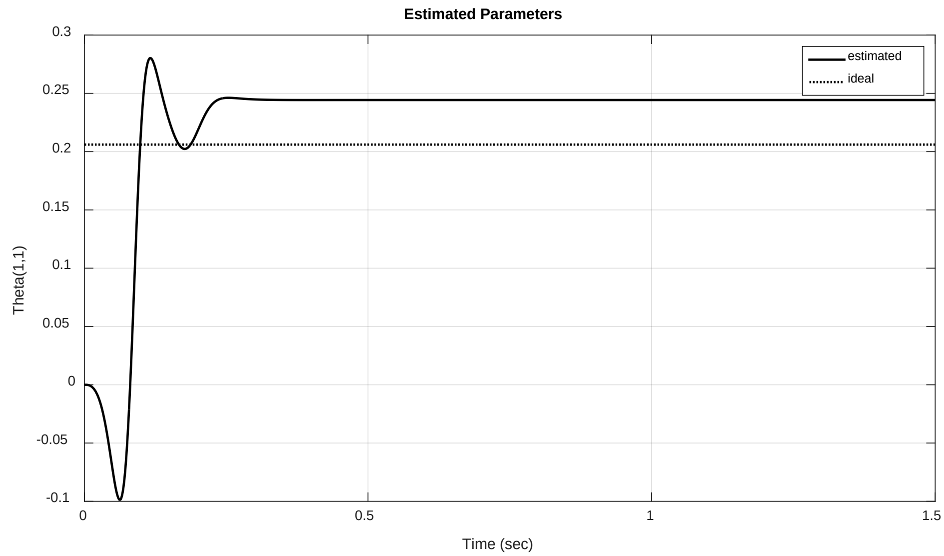

Figure 17 Parameters corresponding to Nonlinear regressor Vector

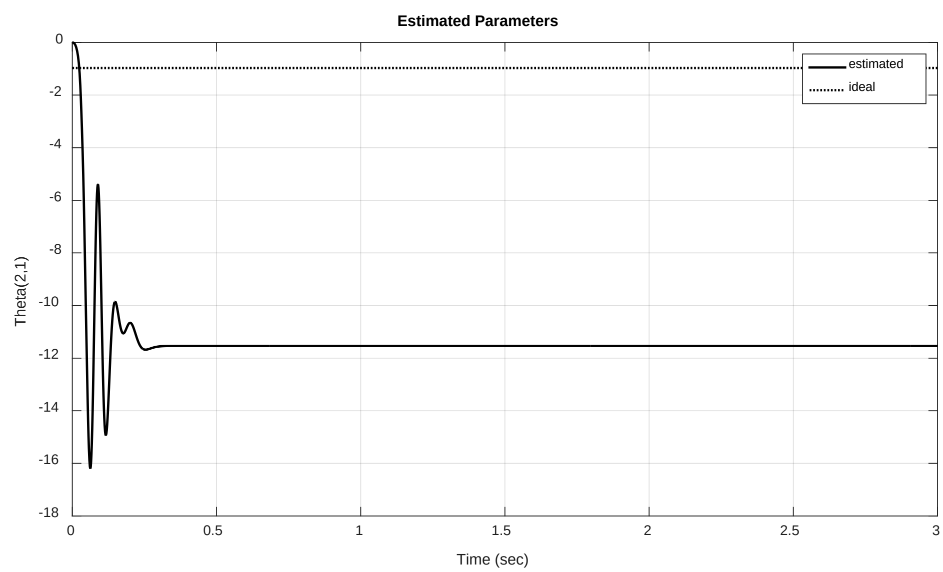

Figure 18 Parameters corresponding to Nonlinear regressor Vector

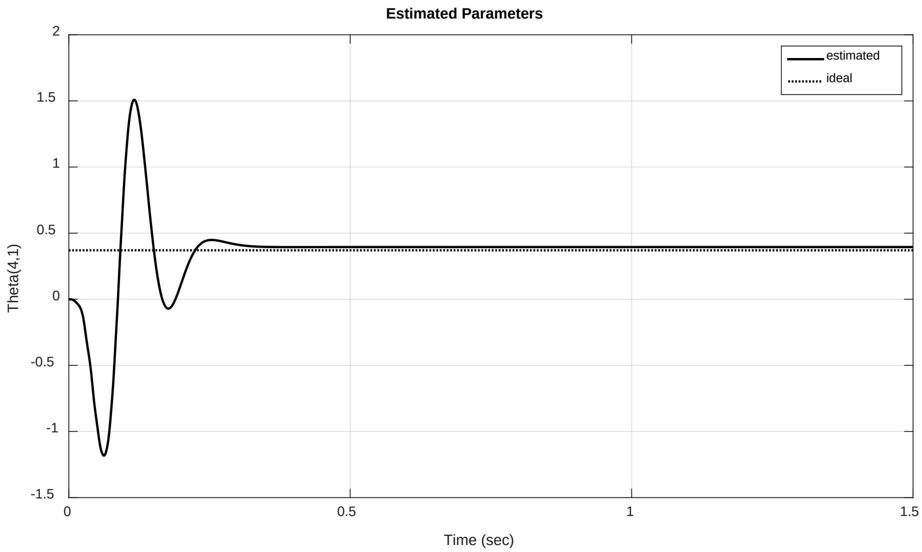

Figure 19 Parameters corresponding to Nonlinear regressor Vector

CHAPTER V

CONCLUSION

A Model Reference Adaptive Control (MRAC) system is designed to stabilize a two-wheeled mobile robot (TWMR), which is modelled as an inverted pendulum. The adaptive controller yields effective results in simulation, achieving bounded control signals and asymptotic output tracking.

The controller was implemented in real-time on a prototype TWMR platform, and it succeeded in maintaining it in the upright position, and prevented it from tipping over even

when an additional unbalanced load was introduced, which induced an unexpected disturbance to the robot. As in most adaptive controllers, the parameter estimates converge to values, which are not necessarily the true values due to the lack of persistently exciting input signals, but still guarantee asymptotic tracking, even when the system is disturbed with an unknown inertia variation. The obtained results in this work pave the way for investigating robust and adaptive nonlinear control techniques, and how they can be applied to other low-cost platforms that possess limited processing power.

APPENDIX

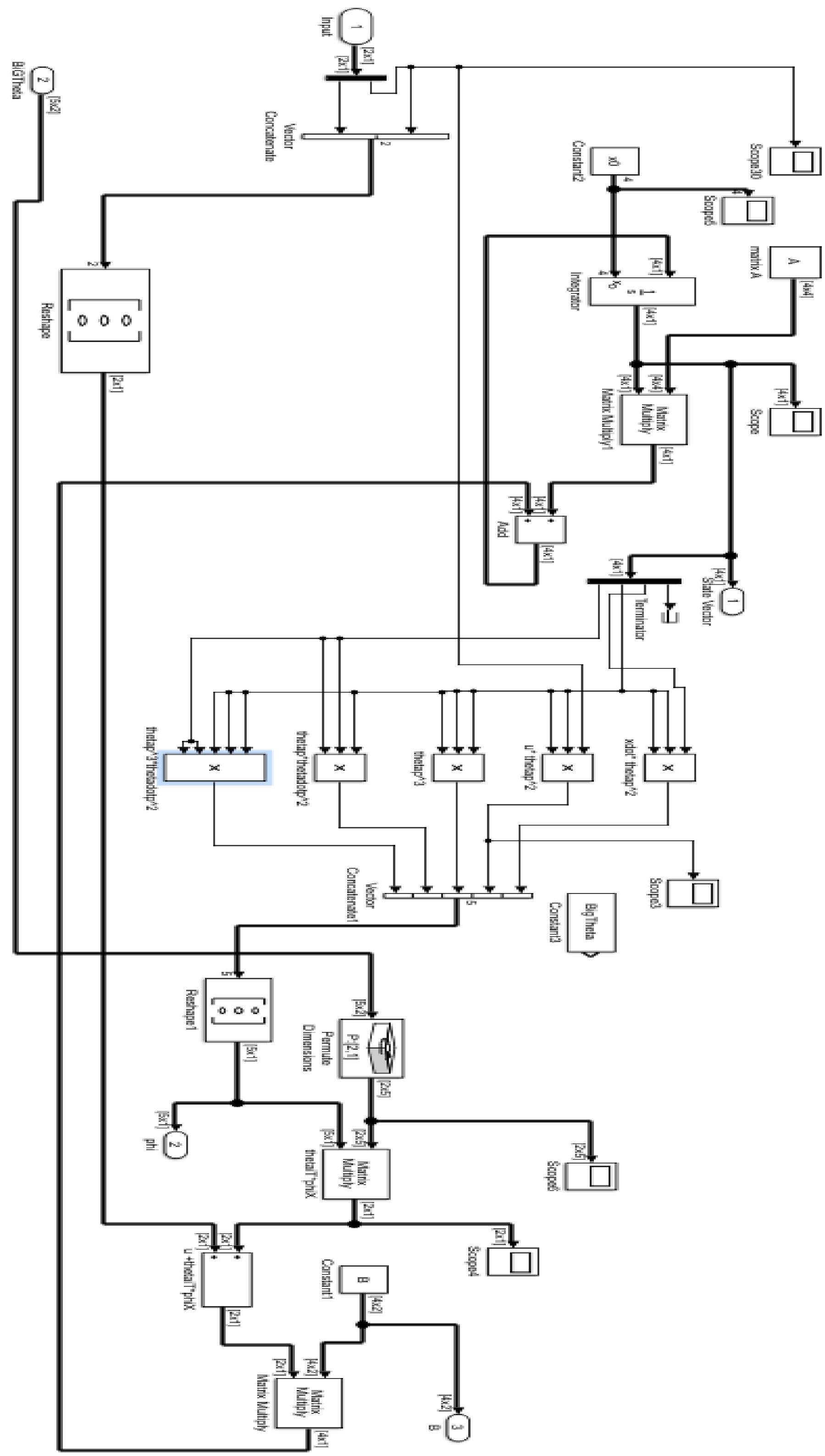

Figure 22 Open Loop Plant

REFERENCES

[1] K. J. Astrom and B. Wittenmark, "Adaptive Control," *Dover,* no. Second Edition, 2008.

[2] Baloh, Michael and Michael Parent, "Modeling and model verification of an intelligent self-balancing two-wheeled vehicle for an autonomous urban transportation system," *The conference on computational intelligence, robotics, and autonomous systems,* pp. 1-7, 2003.

[3] Blankespoor, Adam and Robert Roemer, "Experimental verification of the dynamic model for a quarter size self-balancing wheelchair," *American Control Conference,* pp. 488-492, 2004.

[4] Deng, M., Inoue, A., Sekiguchi, K., & Jiang and L., "Deng, M., et al. "Two-wheeled mobile robot motion control in dynamic environments," *Robotics and Computer-Integrated Manufacturing,* vol. 26, no. 3, pp. 268-272, 2010.

[5] Goher, K. M., M. O., Tokhi and N. H. Siddique., "Dynamic modeling and control of a two wheeled robotic vehicle with a virtual payload," *ARPN Journal of Engineering and Applied Sciences,* vol. 6, no. 3, pp. 7-41, 2011.

[6] Nguyen, Cong Huu and Kien Ngoc Vu, "Applying order reduction model algorithm for balancing control problems of two-wheeled mobile robot," *Industrial Electronics and Applications (ICIEA), 2013 8th IEEE Conference on. IEEE,* pp. 1302-1307, 2013.

[7] Xu, Changkai, Ming Li and Fangyu Pan, "The system design and LQR control of a two-wheels self-balancing mobile robot," *Electrical and Control Engineering (ICECE), 2011 International Conference on. IEEE,* pp. 2786-2789, 2011 .

[8] Jones, Daniel R. and Karl A. Stol, "Modelling and stability control of two-wheeled robots in low-traction environments," *Australasian Conference*

on Robotics and Automation, 2010.

[9] Tsai, Ching-Chih, H. Hsu-Chih and L. Shui-Chun, "Adaptive neural network control of a self-balancing two-wheeled scooter," *IEEE transactions on industrial electronics*, vol. 57, no. 4, pp. 1420-1428, 2010.

[10] Pathak, Kaustubh, Jaume Franch and Sunil KumarAgrawal, "Velocity and position control of a wheeled inverted pendulum by partial feedback linearization," *IEEE Transactions on robotics* , vol. 21, no. 3, pp. 505-513, 2005.

[11] S. C. Lin and C. C. Tsai, "Development of a Self-Balancing Human Transportation Vehicle for the Teaching of Feedback Control," *IEEE Transactions on Education*, vol. 52, no. 1, pp. 157-168, 2009.

[12] Salerno, Alessio and Jorge Angeles, "The control of semi-autonomous two-wheeled robots undergoing large payload-variations," *Robotics and Automation, 2004. Proceedings. ICRA'04*, vol. 2, pp. 1740-1745, 2004.

[13] Salerno, Alessio and Jorge Angeles, "On the nonlinear controllability of a quasiholonomic mobile robot," *Robotics and Automation, 2003. Proceedings. ICRA'03*, vol. 3, pp. 3379-3384, 2003.

[14] E. Lavretsky and K. A. Wise, "Robust and Adaptive Control," *Advanced Textbooks in Control and Signal Processing*, vol. Book, 2013.